FUDMA Journal of Sciences (FJS)
ISSN online: 2616-1370
ISSN print: 2645 - 2944
Vol. 6 No. 2, April, 2022, pp 144 - 155
DOI: https://doi.org/10.33003/fjs-2022-0602-718

ADSORPTION AND ANTICORROSION PROPERTIES OF MILD-STEEL TREATED 2-[(3-HYDROXYLPYRIDIN-2-YL) AMINO] NAPHTHALENE-1,4-DIONE SCHIFF BASE IN 1M-HCL SOLUTION: SYNTHESIS, EXPERIMENTAL AND COMPUTATIONAL STUDIES

[1]Festus Chioma, [1,2]Sorbari Keerabana, *[2]Odozi Nnenna W.

[1]Inorganic Unit, Department of Chemistry, Ignatius Ajuru University of Education, P.M.B. 5047 Rumuolumeni, Port Harcourt, Rivers State Nigeria.
[2]Physical Chemistry Unit, Department of Chemistry University of Ibadan, Oyo State, Nigeria

*Corresponding authors' email: nw.odozi@gmail.com

ABSTRACT
The title Schiff base LH obtained by the reflux condensation of 2-hydroxy-1,4-napthoquinone and 2-amino-3-hydroxypyridine has been characterized via conventional procedures. Adsorption and corrosion inhibition potentials of LH were examined by considering its inhibitory efficiency on mild steel in 1M HCl via weight loss assessment, scanning electron microscopy and density functional theory. Analytical and spectroscopic methods corroborate the bidendate ketoimine-tautomeric assemblage of LH and its stability at ambient temperature. The weight loss measurement was performed at mixt temperatures of 303-343 K and inhibitor concentrations of $1x10^{-5}$ M- $9x10^{-5}$ M with immersion period of 5 h. Higher efficiency of 94.6% was attained with an inhibitor concentration of $9x10^{-5}$ M at 303 K. The adsorption of LH on mild steel (ms) was found to conform with Langmuir absorption isotherm model, while free energy of adsorption showed a spontaneous physiosorption. The computed activation energy (E_a) along other thermodynamic parameters (ΔS and ΔH) was consistent with the latter. The SEM results revealed that the ms superficial was smooth with the inhibitor compared to the ms superficial without the inhibitor indicating inhibition of corrosion of the ms by establishing a layer of protection on the surface. The density functional theory result was in agreement with experimental results.

Keywords: Schiff base, hydroxypyridine, physiosorption, adsorption and corrosion

INTRODUCTION

Corrosion is the chemical dilapidation of metallic substances when wide-open to the surroundings (Akhmetov *et al.,* 1989). It is a process through which the electrochemical oxidation of the metallic substances in reaction with the environment takes place due to oxidant species such as oxygen, sulfur, found in the environment (Zhifeng *et al.,* 2018). Corrosion is a redox reaction in which an oxide of the thin outer coating is molded on the surface of the materials undergoing the reaction (ASM, 2000). Owing to the degradation of metallic substances through corrosion, corrosion inhibitors are designed as one of the most experimental techniques to protect against degradation (Festus *et al.,* 2020). Corrosion inhibitor may be any organic or inorganic substance with the capacity to reduce corrosion of materials when exposed to a corroded medium. The formation of inhibitor pellicle on the metallic surface is associated with basic physiochemical behaviour of the molecule interrelated to its reacting sites, electronic compactness of donor, kind of corrosive medium, aromaticity, steric effects, structural assemblage, nature of relationship amid the *p*-orbital of the inhibitors with the *d*-orbital of iron and charge of metallic surface (Machnikova *et al.*, 2008). Consequently, due to the anti-corrosive properties of inhibitors, many industrial and commercial systems need inhibitors to prevent corrosion of metallic substances and enhance their usefulness, effectiveness as well as their shelf life. The main aim of this research is to ascertain the adsorption and anticorrosion properties of 2-[(3-hydroxylpyridin-2-yl)amino]naphthalene-1,4 dione (LH) in acidic medium at different temperatures with a view to determine its suitability as a corrosion inhibitor for ms.

Experimental

Synthesis of 2-(-3 hydroxylpiridin-2-ylamine) naphthalene-1,4-dione

The inhibitor, LH was synthesized with a technique comparable to that described in the literature (Chioma, 2017). 2-hydroxy-1,4-napthoquinone (2500 mg, 0.0144 mmol) and 2-amino-3-hydroxypyridine (1350 mg, 0.0144 mmol) were measured into the reaction quick-fit flat-bottom flask. Ethanol (15 mL) and a catalytic amount of glacial acetic were added into the mixture and refluxed for 4-5 h. Afterward cooling in ice, the reaction mixture was filtered, recrystallized to give the Schiff base and dried in a vacuum desiccator over calcium chloride. Chemical structural assemblage plus nomenclature for the LH were obtained separately via ISIS-draw and Chem-draw.

METHODS

The synthesized LH remained assessed for solubility in organic and inorganic solvents. The melting point was obtained via a Barnstead Electrothermal IA9100 device on the synthesized ligand. The micro-analysis for synthesized Schiff base was obtained on Perkin-Elmer 7300 DV plus Leco, CHNS-932 elemental analyzers. Transmission infrared spectrum stood acquired on a Schimadzu FTIR-8201 PC spectrophotometer as triple-fold scans via KBr disc routine from 4000 to 350 cm^{-1}, whereas the electronic spectra were recorded amid 190-900 nm scan range on Lambda 25 UV/visible spectrophotometer.

Sample Preparation

The ms were acquired from Ken Johnson Limited, Akwa-Ibom State, cut into coupons (4cm×4cm) for weight loss (WL) measurement and SEM studies. The ms was degreased in ethyl-alcohol, rinsed in $CH_3(C=O)CH_3$, air-dried and kept

in a desiccated desiccator without further polishing (Ituen *et al.,* 2017). The ms is made of C = 0.07%, P = 0.08%, Mn = 0.34%, Si = 0.026%, Cr = 0.05%, Ni = 0.05%, Al = 0.023%, Cu = 0.135%, and Fe = 99.51%. Testing electrolyte of 0.5 M HCl aqueous solution was prepared from Analar Grade 35.4% hydrochloric acid using distilled H_2O. All measurements were performed thrice to acquire a satisfactory reproducibility.

Weight Loss Measurement

This triplicate and conventional method involve the weighing of samples before immersion and re-weighing after duration of a predetermined period (Odozi *et al.,* 2020; Festus and Wodi, 2021). The ms sheets of dimension 4.0 cm×4.0 cm were weighed and wholly immersed in 90 mL of HCl solution at varied concentrations of $1x10^{-5}$ M, $3x10^{-5}$ M, $5x10^{-5}$ M, $7x10^{-5}$ M, and $9x10^{-5}$ M with and without the studied inhibitor, LH. The temperatures of 303 K, 313 K, 323 K, 333 K, and 343 K were maintained in the thermostated water bath for 5 h, after which, the ms was removed from the test solution, dipped in NaOH containing Zinc dust, washed in soapy water using a bristle brush, rinsed in ethanol, dehydrated in $CH_3(C=O)CH_3$, and weighed again. The WL stood calculated from the variance in the mass of the ms before and after immersion into the corrosion environment. The corrosion rates (CR) and the inhibitory competencies were computed via the following relations.

$$CR = \frac{W_0 - W_1}{A \times t} \ (gm^{-2}h^{-1}) \quad (1)$$

$$\% IE = \frac{CR_{blank} - CR_{inh}}{CR_{blank}} \times 100 \quad (2)$$

Scanning Electron Microscopy (SEM) Evaluation

A Q150R ES model was adopted for analyzing the structure of the ms surface, removed from 1M HCl with and without the inhibitor. The sample was put on a metal blunt and spot with gold to enhance conductivity, the images were obtained at a voltage of 15KV using different dimensions at 303 K for 6 h.

Computational and Theoretical Study

Full optimization was acquired for the inhibitor molecule using DFT technique (Festus *et al.,* 2021) at the hybrid functional Becke 3 Lee Yang Par (B3LYP) level of concept on 6-31G (D) source set by Spartan 14 (version 1.2.0) program. It was used to calculate molecular properties, explaining the global reactivity of the inhibitor compound, i.e. HOMO, LUMO, ionization energy (I), electron affinity (A), energy gap (ΔE), electronegativity (χ), softness (σ), hardness (η), nucleophilicity (ε), electrophilicity index (ω), and the number of electrons transferred (Δ*N*).

Generally, DFT calculations have offered a good understanding of molecular properties and enhanced the explanation of the atoms' interactions in molecules. DFT techniques increasingly have been useful, especially in their orrectness and less calculation time; giving vital information about chemical reactivity and selectivity of χ, η, σ, and ΔE. Hence, for an *N*-electron scheme bearing entire electric energy (*E*) plus an external potential ($v_{(r)}$); chemical potential (ρ) branded as the negative of χ, is given as

$$\chi = -\rho = -(\partial E/\partial N)_{v(r)} \quad (3)$$

Hardness is given as

$$\eta = (\partial^2 E/\partial N^2)_{v(r)} = (\partial \rho/\partial N)_{v(r)} \quad (4)$$

The electrons transferred from the inhibitor to the metallic surface may be estimated from Eq. (5)

$$\Delta N = \chi_{Fe} - \chi_{inh}/2(\eta_{Fe} + \eta_{inh}) \quad (5)$$

The *I* and *A* are given as

$$I = -E_{HOMO} \quad (6)$$

$$A = -E_{LUMO} \quad (7)$$

The χ and η can be obtained from the *I* and *A* as shown below:

$$\chi = I + A/2 = -E_{LUMO} + E_{HOMO}/2 \quad (8)$$

$$\eta = I - A/2 = -E_{LUMO} - E_{HOMO}/2 \quad (9)$$

Electrophilicity measures the stabilization in energy as a consequence of more electronic charge ΔN and is expressed as:

$$\omega = \chi^2/2\eta = \rho^2/2\eta \quad (10)$$

The ε is expressed as

$$\varepsilon = 1/\omega \quad (11)$$

$$\sigma = 1/\eta \quad (12)$$

The change in energy is expressed as

$$\Delta E_{back-donation} = -\eta / 4 \quad (13)$$

RESULTS AND DISCUSSION

Synthesis

The Schiff base, LH has been synthesized in a 1:1 reactive ratio amid 2-hydroxy-1,4-napthoquinone and 2-amino-3-hydroxypyridine in ethanolic solution afforded through reflux process. Both analytical plus spectral data substantiated the structural assemblage of the synthesized ligand. The latter exhibited intensive shade and an unchanging micro-crystal nature. The elemental analysis figures corroborate a 1:1 bonding stoichiometric ratio for the synthesized Schiff base. The experimental data remained strongly consistent with hypothetical data and conformed to the suggested structural assemblage for the synthesized ligand. The structure of LH is shown in Figure 1.

Spectral Analysis

Substantial vibrational bands were tentatively apportioned on comparison with documented reports on comparable structures (Bhawsar *et al.,* 2012; Festus *et al.,* 2019). The FTIR spectrum of the Schiff base gave a broadband at 3493 cm^{-1} consistent with intramolecular hydrogen bonding vibration amid the secondary amide proton and ketonic oxygen atom usually observed in ketoimine tautomeric Schiff bases (Festus, 2017). The band (υ_{O-H}) appeared around 3357cm^{-1} within the spectrum confirming the non-dehydration of the hydroxyl-pyridine moiety to give the LH-ligand bearing NH as well as OH vibrations. The medium band, a consequence of C-H moiety stretching vibrations of the (Ar–H) group appeared at 3118 cm^{-1}. Additionally, the distinguishing stretching bands of C=N and C=C moieties were noticed as sole bands in the Schiff base spectrum at 1611 cm^{-1} and 1595 cm^{-1} singly (Osowole and Festus, 2013). The

bands at 1413 cm^{-1} and 1272 cm^{-1} within the spectrum of LH ligand were significantly apportioned to $\nu_{(C=O)}$ plus $\nu_{(C-O)}$, while the absorption bands at 1294, 1015 and 778 cm^{-1} in the LH spectrum stood attributed to (C-N), $\nu_{(C-C)}$ plus $\delta_{(C-O)}$ vibrations individually (Osowole and Festus 2015). The ultraviolet spectrum of the Schiff base displayed intra-ligand bands of $\pi*\leftarrow$n plus $\pi*\leftarrow\pi$ merely as no *d-d* or L→MCT transitions were anticipated. The co-joined dual bands noticed at 33817 and 33532; and 25211 and 25431 cm^{-1} were ascribed to π-π* in addition to n-π* transitions in the LH structural assemblage (Kpee *et al.,* 2018; Abel-Olaka *et al.,* 2019).

Weight Loss (WL) Measurement

The result of CR and %IE acquired from the WL measurement for the mixt concentration of LH in 1M HCl solution at varied T are obtainable in Table 1. It was detected that the CR declines with upsurge in the concentration of the inhibitor plus upsurges in T. This denotes that as the concentration of the inhibitor rises, there is a corresponding rise in the number of adsorption of the inhibitor constituents onto the surface of the ms which hinders corrosion; whereas as the T rises, there is a rise in desorption process hence increasing CR. The %IE increased as the concentration of LH increased. This correlates to the rise in the fraction of the ms surface enclosed by the adsorbed constituent LH as its concentration increases. It was also observed from Fig 2 that the dissolution activities of ms in 1M HCl solution comprising varied concentration of LH at different T, the IE lessened as T improved from 303-343 K for the ms in acidic medium, this revealed that at greater T, the dissolution of ms predominates inhibitor adsorption. As the T of both the uninhibited and inhibited solution increased, CR increased and IE decreased as a result of weakening of physical adsorption (Güvenç, 2018).

Table 1: Corrosion parameters acquired from ms-WL in 1M HCl at varied concentration of LH

Concentration ($moldm^{-3}$)	303K		313K		323K		333K		343K	
	% IE	CR ($gm^{-2}h^{-1}$)	% IE	CR ($gm^{-2}h^{-1}$)	% IE	CR ‘ ($gm^{-2}h^{-1}$)	% IE	CR ($gm^{-2}h^{-1}$)	% IE	CR ($gm^{-2}h^{-1}$)
Blank	–	0.02130	–	0.0217	–	0.02278	–	0.02494	–	0.02499
1×10^{-5}	76.0	0.00502	64.2	0.007404	25.5	0.01249	27.7	0.01803	21.8	0.01931
3×10^{-5}	88.0	0.00246	67.3	0.006760	44.8	0.00926	40.3	0.01489	25.2	0.01845
5×10^{-5}	92.5	0.00159	75.4	0.005082	49.8	0.00842	44.0	0.001395	26.1	0.01825
7×10^{-5}	93.5	0.00137	75.8	0.005001	54.1	0.00770	50.7	0.01229	28.5	0.01765
9×10^{-5}	94.6	0.00114	83.1	0.003499	62.5	0.00628	54.8	0.01126	30.5	0.01715

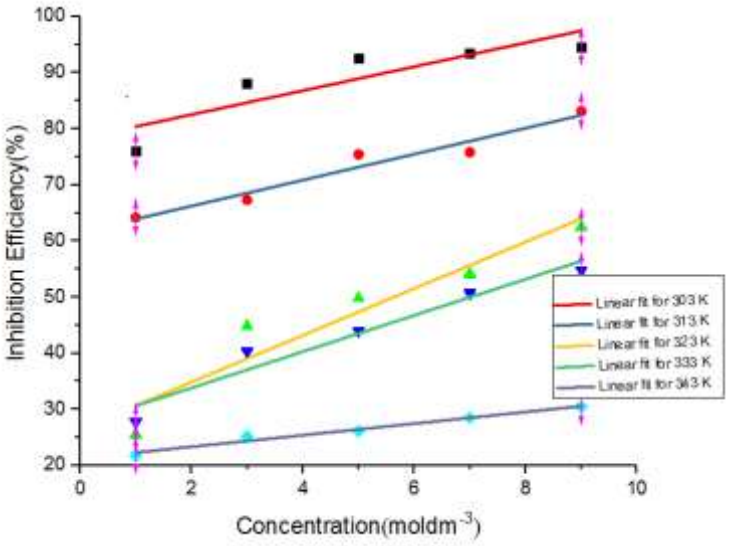

Figure 2**:** The %IE of ms immersed in 1M HCl with mixt concentration of LH

Adsorption Isotherm Models and Adsorption Parameters

The efficiency of LH as an appropriate corrosion inhibitor can be apportioned to the adsorption of molecules via polar functional moieties at the metallic solution interface. The adsorption results from the interaction between either the single pairs of electrons on the heteroatoms or the conjugated double bond or both present in LH and the *d*-orbital of the iron ms. The adsorption of inhibitor molecules on metallic surfaces and interaction amid them is explained via adsorption isotherms. Different adsorption isotherms are used for interpreting various research findings (Vadi *et al.,* 2010; Limousin *et al.,* 2007). The models employed in this research work are those suggested by Langmuir, Temkin, Freundlich plus the thermodynamic/kinetic model. The dissimilar adsorption isotherms with regression coefficient (highest) stood adopted to evaluate the superlative isotherm, which is used to describe the inhibitor adsorption mechanism. The figures remained best described by Langmuir with the highest regression coefficient, R^2 close to 1.

The LH adsorption mechanism was fitted into Langmuir adsorption isotherm model. The Langmuir isotherm is expressed (Ituen et al., 2013) according to Eq. (14)

$$C/\theta = 1/K_{ads} + C \qquad (14)$$

A plot of C/θ against C is shown in Fig3. The associated adsorption factors stood determined from the slope or intercept or both, the thermodynamic function which defined the nature of the inhibitor – metal interaction was also deduced and the results are shown in Table 2a. K_{ads} decreased as the T increased designating adsorption–desorption at lower and greater T for the inhibitor respectively, Shaban et al., (Shaban *et al.,* 2015) reported that a slope which is greater than unity obtained from Langmuir isotherm implied that one or more of each of inhibitor unit takes more adsorption portions. A modification of Langmuir equation expressed in Eq. (15) below applies to this condition (Villamil *et al.,* 1999).

$$C/\theta = n/K_{ads} + nC \quad (15)$$

Hence n is obtained from the slope and is presented in Table 2a. It is as a result of non-unity slope, which indicates that there is an interaction of adsorbed species, a factor not accounted for by the Langmuir model. The data presented in Table 2b was fitted into Temkin adsorption isotherm to explain the state of the interactions as expressed in equation (16) below (Ituen *et al.,* 2017).

$$\theta = -1/2aInC - 1/2aInK_{ads} \quad (16)$$

The 'a' is the molecular interaction parameter. Umoren and Ebenso (2007) fitted their experimental data into the Temkin model acquiring non-positive data of all 'a' in all cases and associated it to repulsion that takes place in the adsorbed layer. Employing the Temkin plot of θ versus log C over 303-343K for the inhibitor as shown in Fig 4 and presented in Table 2b, the corrosion inhibitor equilibrium constant and the molecular interaction parameter were obtained. It was observed that the data of 'a' remained negative, which indicated that repulsion, takes place within the absorbed layer. It was also observed that the values of K_{ads} obtained was very high signifying robust adsorption of the inhibitor molecules to the metallic superficial area, the data similarly decreased with an increase in T showing a decline in the rate of condensation of LH on the metallic surface due to high T which enhance desorption process.

The results obtained were also fitted into Freundlich model as presented in Table 2c. The Freundlich expression is shown as

$$Log\ \theta = logK_{ads} + 1/nlogC \quad (17)$$

A plot of log θ against log C remained acquired as presented in Fig 5. The values of 1/n were adopted to explain the simplicity of adsorption. Frequently, when θ is less than 1/n less than 1 adsorption is alleged to be easy, as well as moderate or difficult when 1/n = 1 or 1/n is greater than 1 respectively. Seifzadeh *et al.,* (2013) reported that adsorption is stress-free acquired when θ > n > 1, moderate if n=1 and difficult when n < 1. It has been reported that n is regularly a non-negative constant (Mert *et al.,* 2014; Khadom *et al.,* 2010), which can also be explained as the adsorption intensity (Dada *et al.,* 2012). The reciprocal of n has been designated as a non-homogeneity factor, the lesser the data of 1/n, the larger the anticipated non-homogeneity plus the value of n at 1, and up to 10 specify favourable adsorption procedure. From Table 2c, the inhibitor LH showed the values of n > 1 which indicates favourable or easy adsorption to the metal surface. The K_{ads} obtained shows a decrease as the T increases due to the desorption process dominated by an increase in T.

The Gibb free energy of the above-mentioned inhibitor on ms was examined by the application of the variously mentioned isotherm above and presented in Table 2a, 2b and 2c separately. The Gibb free energy of adsorption ΔG_{ads} is accessible (Shukla and Ebenso, 2011) as

$$\Delta G_{ads} = -2.303RT \log (55.5K_{ads}) \quad (18)$$

Non-positive data of ΔG_{ads} shows that the inhibitor molecules are impulsively adsorbed on the metallic surface, and positive values mean non-spontaneous. The mechanism of adsorption is physisorption when the value of ΔG_{ads} is ≤ -20 KJ/mol and chemisorption when $\Delta G_{ads} \geq$ -40 KJ/mol (El-Sherif and Badawy, 2011). The value amid this sort is typically associated with mixed mechanism occasionally referred to as physiochemisorption (Verma *et al.,* 2016). The negative value of ΔG_{ads} as presented in Tables 2a, 2b and 2c showed the rapid adsorption reaction and the steadiness of the adsorbed layer of the inhibitor on the ms surface. The data of ΔG_{ads} obtained from the Langmuir and Freundlich concepts were ≤ -13 KJ/mol indicating physisorption process. However, the values of ΔG_{ads} obtained from Temkin concept were in between $\Delta G_{ads} \geq$ -40 KJ/mol and $\Delta G_{ads} \geq$ -20 KJ/mol showing mixed mechanism or physiochemisorption process.

Thermodynamic Studies

The influence of T on the corrosion of ms in the presence and absence LH as inhibitor was studied using the Arrhenius concept, relating the CR of the ms and T as shown by Arrhenius equation below and this concept was employed to obtain the activation energy (E_a)

$$\log CR = \log A - E_a/2.303RT \quad (19)$$

The variation of log CR against the reciprocal of T is shown in Fig 6 for the ms in 1M HCl in the presence of LH. The computed values of E_a are given in Table 3. It was observed that there is an increased E_a with the inhibitor at each concentration compared to its lack, indicating that the addition of inhibitor increased the energy of activation that 1M HCl most surpass for it to attack the ms and corrode the ms surface (Ituen et al., 2017). Therefore, it shows that adsorption of LH on ms leads to the formation of a thin protective layer that slows down or hinders the metal activity in the

Table 2a: Adsorption parameters for LH on ms in 1M HCl obtained at mixt T (Langmuir isotherm)

T(K)	Slope	R^2	N	K_{ads}	ΔG_{ads} (KJmol^{-1})
303	1.02367	0.9999	1.02	3.249	-13.08
313	1.16613	0.9892	1.17	1.405	-11.33
323	1.35998	0.9809	1.36	0.431	-8.54
333	1.59945	0.9840	1.60	0.394	-8.52
343	3.12494	0.9889	3.12	0.357	-8.51

Table 2b: Adsorption parameters for LH on ms in 1M HCl obtained at mixt T (Temkin isotherm)

T(K)	Slope	R^2	a	K_{ads}	ΔG_{ads} (KJmol^{-1})
303	0.08640	0.95552	-5.78	7.4×10^{8}	-50.45
313	0.07986	0.80709	-6.26	9.6×10^{5}	-39.88
323	0.15754	0.97442	-3.17	5.1×10^{5}	-32.66
333	0.11949	0.97573	-4.18	3.2×10^{7}	-33.66
343	0.03690	0.91671	-13.55	2.4×10^{8}	-31.42

Table 2c: Adsorption parameters for LH on ms in 1M HCl obtained at varied T (Freundlich isotherm)

T(K)	**Slope**	**R^2**	**n**	**K_{ads}**	**ΔG_{ads} (KJmol^{-1})**
303	0.10171	0.94469	9.83	2.48	-12.40
313	0.11061	0.83314	9.04	2.23	-12.53
323	0.39065	0.96404	2.56	2.07	-12.74
333	0.30481	0.98870	3.28	1.86	-12.83
343	0.14407	0.94498	6.94	1.13	-11.80

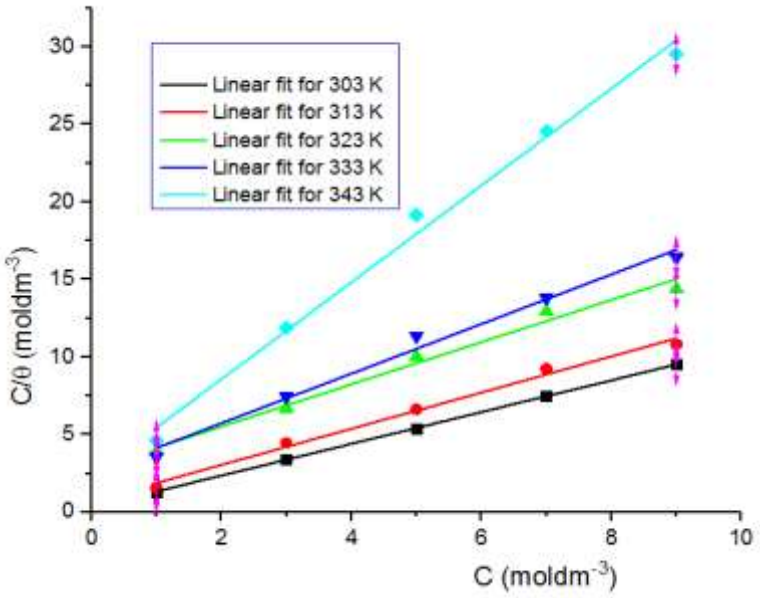

Figure 3**:** Langmuir adsorption isotherm plot for ms in 1M HCl with mixt concentration of LH at varied T

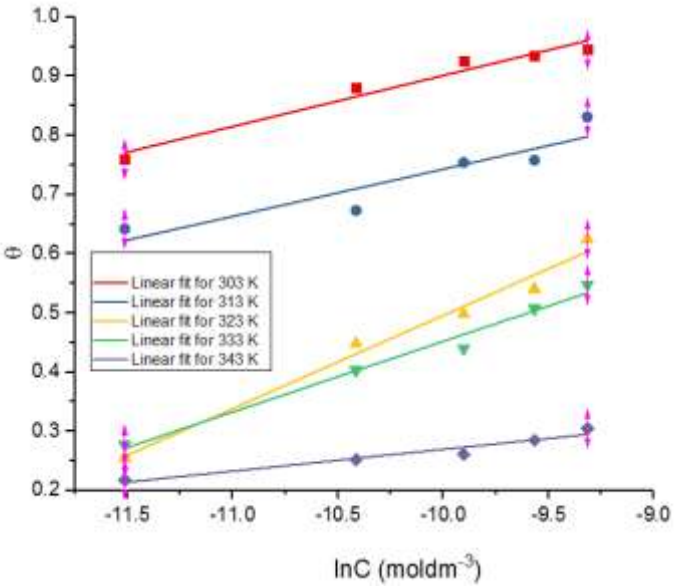

Figure 4**:** Temkin adsorption isotherm plot for ms in 1M HCl with varied concentration of LH at mixt T

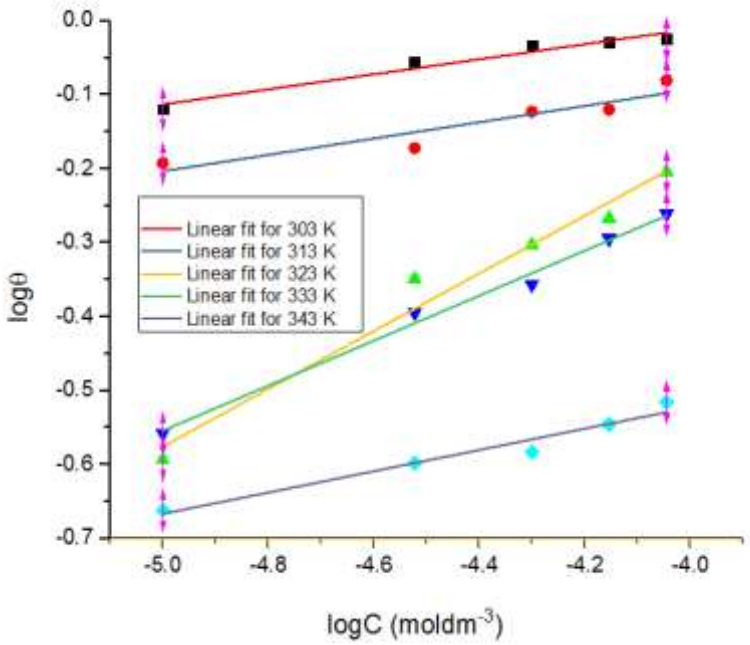

Figure 5**:** Freundlich adsorption isotherm plot for ms in 1M HCl with mixt concentration of LH at varied T

electrochemical reaction of corrosion (Obi-Egbedi and Obot, 2013). It stood detected that rise in E_a for the corrosion reaction implied that LH would be more efficient at lesser T, which is in harmony with the noticed fashion of IE with T plus the stated physisorption mechanism for the adsorption of the inhibitor (Ulaeto *et al.*, 2012). Thermodynamic quantities such as enthalpy change (ΔH_{ads}) plus entropy change (ΔS_{ads}) were also obtained from the Eyring transition state equation

$$\text{Log } CR/T = \log (R/Nh) + (\Delta S/2.303R) - (\Delta H/2.303RT) \quad (20)$$

A conventional line graph was acquired from the plot of log CR/T against 1/T as presented in Fig 7, with slope (-ΔH/2.303R) and intercept (logR/hN + (ΔS/2.303R)). The computed data of ΔH_{ads} and ΔS_{ads} obtained from this plot are accessible in Table 3. The positive data of ΔH_{ads} both with and without the inhibitor reflects the endothermic state of the ms dissolution reaction, i.e. indicated that the dissolution of ms is challenging. The large negative data of ΔS_{ads} for ms in 1M HCl implied that the activated complex serves as the rate determining step and is association instead of dissociation step. With the inhibitor, the data of ΔS_{ads} increased but was interpreted as a rise in entropy (disorderliness) converting the reactants to activated complexes (Abiola and James 2009). The positive values of ΔS_{ads} showed that the adsorption process is accompanied by a proliferation in entropy that forms the propelling potency for the adsorption of the inhibitor onto the ms surface.

Table 3: Thermodynamic parameters determined from Arrhenius plot

Concentration ($moldm^{-3}$)	**E_a ($KJmol^{-1}$)**	**ΔH ($KJmol^{-1}$)**	**ΔS ($Jmol^{-1}K^{-1}$)**
Blank	0.471	0.353	–75.95
1×10^{-5}	3.694	7.770	2.82
3×10^{-5}	4.979	10.73	34.22
5×10^{-5}	6.360	13.28	61.65
7×10^{-5}	6.519	13.59	64.52
9×10^{-5}	6.790	14.91	78.08

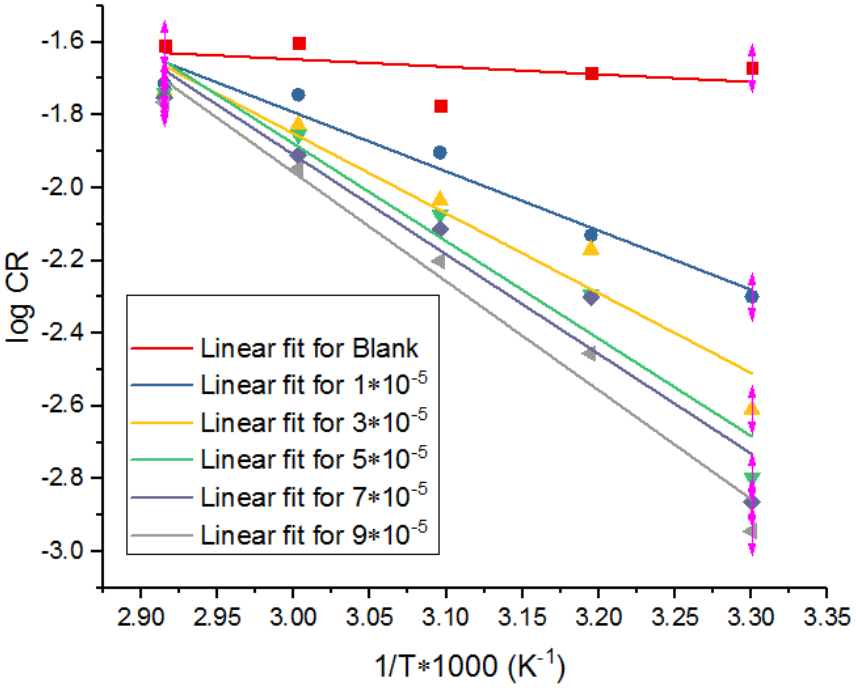

Figure 6**:** Arrhenius plot for the corrosion of ms in 1M HCl at mixt concentrations of LH

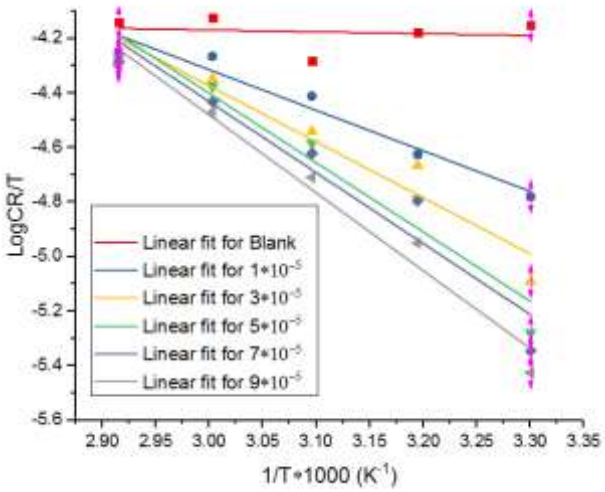

Figure 7**:** Transition state plot for the corrosion of ms in 1M HCl at mixt concentrations of LH

Scan Electron Microscopy

The SEM micrographs of ms with and without the inhibitor, and in a solution of 1M HCl are presented in Fig 8. Fig. 8a revealed that the ms sample at 1500x magnification before immersion was smooth but on immersion of the ms in 1M HCl without inhibitor (Fig 8b) flakes due to corrosion of the ms was observed an indication that the surface was highly spoiled. In the presence of the inhibitor on ms, (Fig 8c) the damaging effect of the acid on the metallic sample was greatly reduced giving a more ordered corrosion product as surface coatings. Also, the surface of the ms (Fig 8c) remained modified by the inhibitor as a result of the shielding layer formed by the inhibitor on the ms [32]. A highly corroded superficial structure is detected after immersion in the uninhibited systems, base on the corrosive attack of the acid solution as shown in Fig. 8b. With the addition of inhibitor (Figures 8c), the corrosion damage was reduced, showing that this compound subdued the corrosion of ms to different degrees through the mechanism of physical adsorption (Oguzie *et al.*, 2012).

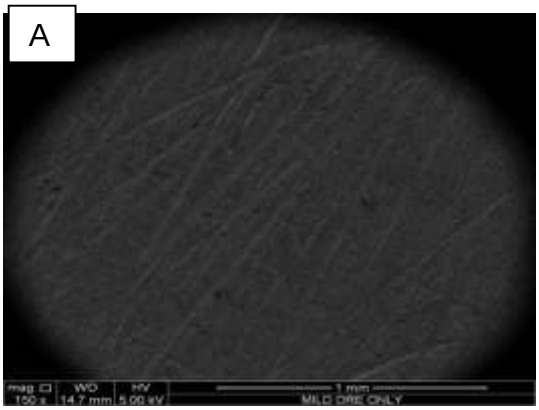

SEM micrograph of ms alone at 1500x

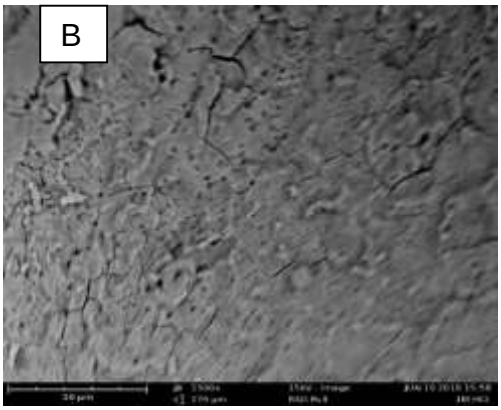

SEM micrograph of ms in 1M HCl at 1500x

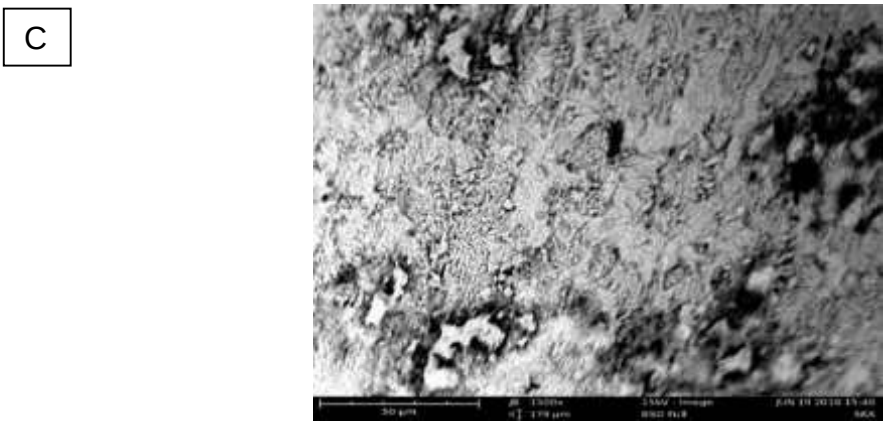

SEM micrograph of ms in the inhibitor at 1500x

Figure 8**:** Scanning electron micrographs of ms only (A), ms in 1M HCl (B), and ms with the inhibitor (C)

Global Descriptors

The optimized molecular assemblages, molecular electrostatic potentials (ESP), HOMO and LUMO of the studied inhibitor molecule are accessible in Fig. 5. Quantum chemical calculation is a very crucial tool in presenting the relationship amongst molecular assemblages and corrosion IE. Accordingly to Fukui's principle, the movement of electron was based on the interface amid HOMO and LUMO interacting atoms. E_{HOMO} is a quantum chemical parameter that reveals the potency of a molecule to donate electron. Therefore, it has been reported that inhibitors, which have greater values of E_{HOMO}, are liable to give electrons to an acceptor that has an unfilled molecular orbital that is low in energy. Contrarily, the E_{LUMO} measures how much the molecule receives electrons. Hence when a molecule receives more electrons there is a corresponding decrease in the value of E_{LUMO} (Festus *et al.,* 2020). Studies showed that the proficiency of an inhibitor increases with a corresponding rise in the values of E_{HOMO} (Popova *et al.,* 2003). The calculated global descriptors are accessible in Table 4. The increased value of E_{HOMO} over $E_{LUMO,}$ validates the inhibitor molecule as a good inhibitor.

Electrophilicity (ω) examines the capability of atoms to receive electrons. Greater value of ω, designates greater ability of the atom or molecule to receive electrons. So, a better nucleophile is associated with small data of ρ and ω; while a better electrophile has great values of ρ. It is obvious in Table 4 that the molecule has a low ω value hence a better nucleophile. Based on ω and ε data contained in Table 4, it is suggested that corrosion IE of the examined compound, agreed with practical data. The number of electrons transferred (ΔN) was likewise computed as shown in Table 4. Value of ΔN revealed that the IE conforms to Lukovits's study (Lukovits *et al.,* 2001). If $\Delta N < 3.6$, then there is an equivalent upsurge in the adeptness of the inhibitor coupled with the proliferating capacity to donate electron to the metallic surface. The result indicates that ΔN value agrees drastically with the laboratory IE. The electron back donation ($\Delta E_{b\text{-}d}$) implies that when $\eta>0$ or $\Delta E_{b\text{-}d}<0$, then back donation occurred. As reported in Table 4, the results indicate that $\Delta E_{b\text{-}d}$ less than 0, hence the charge transfer accompanied by back-donation from the molecule is likely to occur (Obot *et al*., 2010). The η and σ are crucial properties which are associated with the molecular stability and as well as reactivity (Lukovits *et al.,* 2001) revealed that hardness basically shows the agitation of the molecules, ions or atoms towards destruction of their electron cloud when the chemical reaction is perturbed. Meanwhile, a hard molecule possess a large energy gap but a soft molecule exhibits a small energy gap. Consequently, when a molecule has a small data of global hardness, the molecule is anticipated to be a suitable corrosion inhibitor. A soft molecule is adsorbed readily onto the metallic surface than a hard molecule. Therefore, the higher the adsorption of a molecule, the greater the softness, and the lower the η of the molecule. Table 4 presents the computed value of η for the studied inhibitor molecule. It was pointed out by (Guo *et al.,* 2014) that an inhibitor with the highest figure of IE exhibits a greater value of softness and a lower value of η. For the simple transmission of electron, Hasanov *et al.,* (2007) documented that adsorption

takes place at the portion of the molecule with the highest value of softness (σ). The result considered in this study disclosed that the inhibitor displayed a higher value of softness 0.67567eV compared to 0.6246 eV reported in other literature (Şaban *et al.,* 2017). The inhibitor has higher IE. The energy gap (ΔE) of a molecule measures its reactivity. A molecule with a lower energy gap has higher reactivity. Therefore, suitable corrosion inhibitors have lower values of energy gap (Ebenso *et al.,* 2010). The data as indicated in Table 4 confirms that the inhibitor has a low energy gap. Hence, the molecule is a suitable corrosion inhibitor for ms in acidic medium with good IE.

Table 4: Calculated quantum chemical parameter for the inhibitor, LH

Total energy	-912.79264 (au)
E_{HOMO}	-5.69 eV
E_{LUMO}	-2.73 eV
Energy gap (ΔE)	2.96 eV
Dipole moment (μ)	4.70 Debye
Ionization potential (I)	5.69 eV
Electron Affinity (A)	2.73 eV
Electronegativity (χ)	4.21 eV
Hardness (η)	1.48 eV
Softness (σ)	0.67567 eV
Fraction of electrons transferred (ΔN)	0.9426
Nucleophilicity (ε)	0.16700 eV
Electrophilicity (ω)	5.9878 eV
Chemical potential (ρ)	-4.21 eV
Electron back donation (ΔE_{b-d})	-0.37 eV

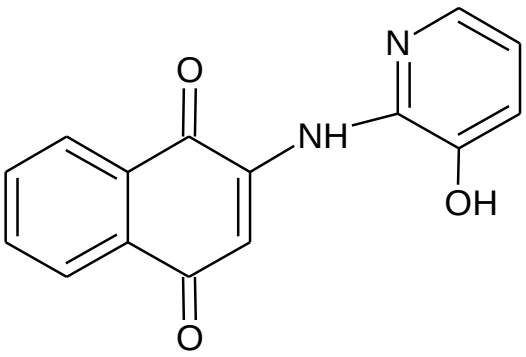

Figure 1: 2-[(3-hydroxypyridin-2-yl)amino]naphthalene-1,4-dione, LH

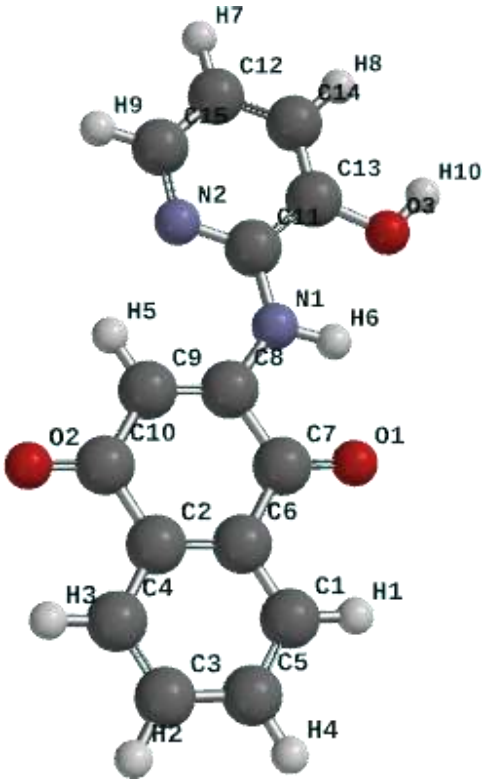

Figure 9a: DFT (B3LYP) Optimized structure of LH

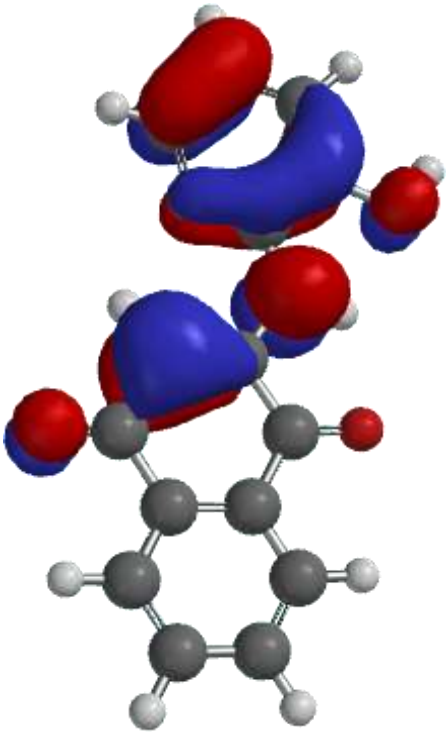

Figure 9b: HOMO orbital diagram of LH

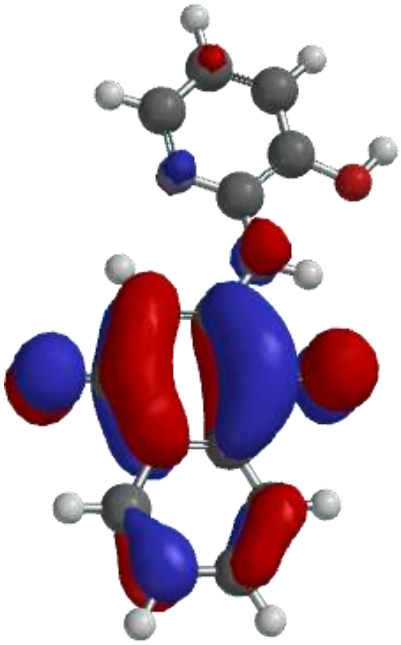

Figure 9c: LUMO orbital diagram of LH

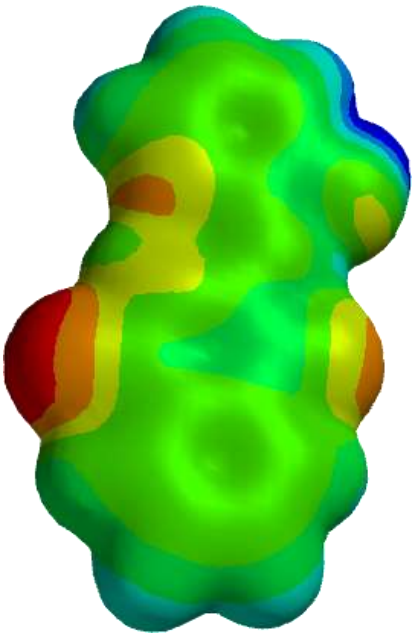

Figure 9d: Electrostatic potential map diagram of LH

CONCLUSION

From our research findings, LH acts as a suitable inhibitor for corrosion of ms in 1M HCl solution. The trends of IE with temperature as well as values of kinetic and activation parameters for corrosion and corrosion inhibition processes point toward spontaneous physisorption of LH on the mild steel surface. The adsorption of LH tailed the Langmuir isotherm model. The morphology of the ms with and without the inhibitor examined using SEM indicated that the surface of the ms in the presence of inhibitor was smoother than that in the absence of the inhibitor, thus adsorption of LH on the ms surface. The DFT- based computation of global parameters confirmed that the inhibitor has a great affinity toward adsorption on the metallic surface and therefore impedes corrosion reaction.

REFERENCES

Abel-Olaka, L. C., Kpee, F. and Festus, C. (2019). Solvent Extraction of 3*d* Metallic Elements using N_2O_2 Schiff Base-Chelators: Synthesis and Characterization. *Nigerian*

Research Journal of Chemical Sciences. 7(2); 133-146. *http://www.unn.edu.ng/nigerian-research-journal-of-chemical-sciences/p2*

Abiola, O. K. and James, A. O. (2009). The effects of *Aloe vera* extract on corrosion and Kinetic of corrosion process of Zinc in HCl solution. *Corrosion Science*, 51, 1879

Akhmetov, B., Novicchenko, Y.V. and Chapurin, V. (1989). Physical and Colloid Chemistry, 1st Edition, Mir Publishers, Moscow, 1989.

ASM International, Understanding the Basis: The effect and economic importance of corrosion, Ohio, 2000.

Bhawsar, J., Jain, P. K. and Jain, P. (2012); Experimental and computational studies of Nicotiana tobacum leaves extract as green corrosion inhibition for mild steel in acidic medium. Alexandria Engineering Journal, 54:769-775.

Chioma, F. (2017). Synthesis, Experimental Characterization; and Antimicrobial, and Antioxidant Studies of some M^{2+} Chelates of Schiff Base Ligand Bearing hydroxypyridine Moiety. *Scholarly Journal of Scientific Research and Essay*. 6(6), 174-180. https://scholarly-journals.com/sjsre/publications/2017/December/toc.htm

Ebenso, E. E., Taner, A., Fatma, K.,Ian, L., Cemil, Ö., Murat, S. and Savıour, A. U. (2010). Theoretical studies of some sulphonamides as corrosion inhibitors for mild steel in acidic medium. *Int. J. Quant. Chem., 110* (2010) *1003-1018.* https://doi.org/10.1002/qua.22430

Dada, A. O., Abiodun, P. O., Ayomadewa, O. and Adewumi, O. D. (2012). Langmuir, Feundlich, Temkin and Dubinin - Radushkevich isotherm studies of equilibrium sorption of Zn2 unto phosphoric acid modified rice Husk. *J. of Appl. Chem*. 3(1):38-45.

El-Sherif, R. M. and Badawy, W. A. (2011). Mechanism of corrosion and corrosion inhibition of tin in aqueous solution containing tartaric acid. *Int. J. Electrochem. Sci.*, 6: 6469.

Festus, C. (2017). Synthesis, Characterization and Antibacterial Studies of Heteroleptic Co(II), Ni(II), Cu(II) and Zn(II) Complexes of N-(2-hydroxybenzylidene)pyrazine-2-carboxamide. *International Journal of Chemistry, Pharmacy & Technology*, 2(5); 202-211

Festus, C., Odozi, W. N. and Olakunle M.. (2020). Preparation, spectral characterization and corrosion inhibition studies of (*e*)-*n*-{(thiophene-2-yl)methylene}pyrazine-2-carboxamide schiff base ligand. *Protection of Metals and Physical Chemistry of Surfaces.* 56(3); 651–662.

Festus, C., Jude, I. A., Collins, U. I. (2021). Ligation Actions of 2-(3-hydroxypyridin-2-ylamino)naphthalen-1,4-dione: Synthesis, Characterization, *In-vitro* Antimicrobial Screening, and Computational Studies. *Indian Journal of Heterocyclic Chemistry*, 31(01); 1-13.

Festus C., Don-Lawson, C. D. and Ima-Bright N. (2019). Synthesis Involving Asymmetric Pyrazine-Schiff Base with Co^{2+}, Ni^{2+} and Cu^{2+} ions: Spectral and Magnetic Characterization; and Antibacterial studies. *Int.l J. of Research & Innovation in Applied Science; 4(4).*

Festus, C. Collins, U. I. and Obinna, O. (2020). Novel 3d divalent metallic complexes of 3-[(2-hydroxy-5-methylphenylimino)-methyl]-napthalen-2-ol: Synthesis, spectral, characterization, antimicrobial and computational studies. *Journal of Molecular Structure* 1210 (2020); 1-13.

Festus, C. and Wodi, C. T. (2021). Corrosion Inhibition; and Antimicrobial Studies of Bivalent Complexes of 1-(((5-ethoxybenzo[d]thiazol-2-yl)Imino)methyl)naphthalene-2-ol Chelator: Design, Synthesis, and Experimental Characterizations. Direct Research Journal of Chemistry and Materials Science, 8(2021); 31-43. https://directresearchpublisher.org/drjcm/vol-8-november-2021/

Gomez, B. N.V., Likhanova, M. A., Dominguez-Aguilar, R., Martinez, A. and Vela, J. L. Gazquez, J. (2006). Phys. *Chem. B* 110 : 8928-8934

Guo, L., Zhu, S., Zhang, S., He, Q. and Li, W. (2014). Theoretical studies of three triazole derivatives as corrosion inhibitors for mild steel in acidic medium. *Corros Sci* 2014; 87: 366–375

Güvenç, G. (2018). Experimental and theoretical study of a novel naphthoquinone Schiff base. *Open chem.* 16*;* 2018-0121

Hasanov R, Sadikoglu M, Bilgic S (2007).Electrochemical and quantum chemical studies of some Schiff bases on the corrosion of steel in H2SO4 solution. *Appl. Surf. Sci.,* 253: 3913-3921

Ituen, E. B., Udo, U. E., Odozi, N. W.and Dan, E. U. (2013). Adsorption and kinetic/themodynamic characterization of aluminum corrosion inhibitor in sulphuric acid by extract of Alstonia boonei *J. of Appl. Chem*. 52-59.

Ituen, E. B., Udo, James, A.O., and Akaranta, O. (2017). Elephant grass biomass extract as corrosion inhibitor for mild steel in acidic medium. *Journal of Material and Environmental Sciences* 8.4:1498-1505.

Khadom, A. A., Yaro, A. S. and Khadum, A. A. H. (2010). Adsorption mechanism of benzothiazole for corrosion inhibition of copper-nickel alloy in hydrochloric acid. *J. Chilean Chem. Soc.* 55:150-152.

Kpee, F., Ukachukwu, C. V. and Festus, C. (2018). Synthesis, Characterization and Extractive Potentials of Aminopyrimidine Schiff Base Ligands on Divalent Metal Ions. *Nigerian Research Journal of Chemical Sciences.* 4(2); 193-203. *http://www.unn.edu.ng/nigerian-research-journal-of-chemical-sciences/193*

Limousin, G., Gaudet, J. P., Charlet, L., Szenknect, S., Barthes, V. and Krimissa, M. (2007). Sorption isotherms: A review on physical bases, modeling and measurement. *Appl. Geochem.*, **22:** 249-275

Lukovits, I., Kálmán, E. and Fabrizio, Z. (2001). Corrosion Inhibitors—Correlation between Electronic Structure and Efficiency. *Corrosion -Houston Tx-* 57(1):3-8 DOI:10.5006/1.3290328

Machnikova, E., Kenton, W. and Hackerman, E. (2008). Corrosion inhibition of carbon steel in hydrochloric acid by furan derivatives. *Electrochimica Acta*, 53(20):6024-6032 ·

Mert B. D., Yuce, A. O., Kardas, G. and Yazici, B. (2014). Inhibition effect of 2-amino-4-methylpyridine on mild steel corrosion: experimental and theoretical investigation. *Corros. Sci.* 85:287-295.

Obi-Egbedi, N. O. and Obot, I. B. (2013). Xanthone; A new and effective corrosion inhibitor for mild steel in sulfuric acid solution, *Arabian, J. of Chem.* 6, 211-223

Obot, I. B. and Obi-Egbedi, N. O. (2010). Adsorption properties and inhibition of mild steel in sulfuric acid solution by ketoconazone: Experimental and theoretical investigation. *Corr. Sci.* 52 198-204.

Odozi, W. N., Festus C. and Muhammad, A. D. (2020). Synthesis, adsorption and inhibition behaviour of 2-[(thiophen-2-ylmethylidene)amino] pyridine-3-ol on mild steel corrosion in aggressive acidic media. *Nigerian Research Journal of Chemical Sciences.* 8,(2); 291-307. http://www.unn.edu.ng/nigerian-research-journal-of-chemical-sciences

Oguzie, E. E., Adindu, C. B., Enenebeaku, C. K., Ogukwe, C. E., Chidiebere, M. A. and Oguzie, L. L. (2012). Natural products for materials protection: Mechanism of corrosion inhibition of mild steel by acid extracts of Piper guineense. *Journal of Physical Chemistry*, Doi.org/10.1021/jp300791s

Osowole, A. A. and Festus, C. (2013). Synthesis, characterization and antibacterial activities of some metal(II) complexes of 3-(-1-(2-pyrimidinylimino)methyl-2-napthol. *Elixir Appl. Chem. 59 (2013) 15843-15847*

Osowole, A.A. and Festus, C. (2015). Synthesis, characterization, antibacterial and antioxidant activities of some heteroleptic Metal(II) complexes of 3-{[-(pyrimidin-2-yl)imino]methyl}napthalen-2-ol. Journal of Chemical, Biological and Physical Sciences. 6(1); 080-089.

Popova, A., Sokolova, E., Raicheva, S. and Christov, M. (2003). AC and DC study of the temperature effect on mild steel corrosion in acid media in the presence ofbenzimidazole derivatives. *Corrosion Science*, 45(1): 33-58.

Şaban, E., Zaki, S., Safi, S., Dilara, Ö. and LeiGuo, C. K. (2017) A computational study on corrosion inhibition performances of novel quinoline derivatives against the corrosion of iron. *Journal of molecular scienc*e. 751-761.

Seifzadeh, D., Basharnawaz, H, Bezaatpou A. (2013). A Schiff base compound as effective corrosion inhibitor for magnesium in acidic media. Mater. *Chem. Phys*. 138:794-804.

Shaban, S. M., Aiad, I., El-Sukkary, M. M., Soliman, E. A. and El-Awady, M.Y. (2015). Inhibition of mild steel corrosion in acidic medium by vanillin cationic inhibitor. *J. Mol. Liq.* 203: 26-28.

Shukla, S. K. and Ebenso, E. E. (2011). Corrosion inhibition, Behaviour and thermodynamic properties of streptomycin on mild steel in hydrochloric acid medium. *Int. J. Elechem Sci.* 6: 3281-3286

Ulaeto, S. B., Ekpe, U. J., Chidiebere, M. A. and Oguzie, E. E. (2012). Corrosion inhibition of mild steel in hydrochloric acid by acid extract of *Eichhornia crassipes. Intl J. of Material and Chem.*,2(4):158-164

Umoren, S. A. and Ebenso, E. E. (2007). The synergistic effect of polyacrylamide and iodided ions on the corrosion of mild steel in H_2SO_4. *Materials Chemistry and Physics*, 106: 387-393.

Vadi, M., Abbasi, M., Zakeri, M. and Yazdi, J. (2010). Application of the Freundlich, Langmuir, Temkin and Harkins-Jura adsorption isotherms for some amino acida and amino acdis complexation with manganese (ii) on carbon nanotube. Proceedings of International Conference of Nanotechnology and Biosensors. *Journal. Phys. Theor. Chem* 7(2):95-104

Verma, C., Singh, P. and Quraishi, M. A. (2016). A thermodynamic, electrochemical and surface investigation of Bis(indolyl) methanes as green corrosion inhibitors for mild steel in 1M HCl acid solution. *J. Asso. Arab Univ. Bas. Appl. Sci*., 21: 24-30

Villamil, R. F. V., Corio, P., Agostinho, S. M. L. and Rubim, J. C. (1999). Effect of sodium dodecylsulphate on copper corrosion in sulphuric acid media in the absence and presence of benzotriazole. *J. Electroanalytical Chem*, 472(2): 112-9.

Zhifeng, Z., Fengjuan, W., Yao, L., Shengping, W., Weihua, L., Wei, S., Dong, G. and Jinyang, J. (2018) Molecule adsorption and corrosion mechanism of steel under protection of inhibitor in a simulated concrete solution with 3.5% NaCl. *RSC Adv.*, 8(20648). DOI: 10.1039/c8ra03235a